

Determination of Diffusion and Dispersion Parameters for Flow in Porous Media

Iichiro KOHNO* and Makoto NISHIGAKI*

(Received September 22, 1981)

Synopsis

The purposes of this research is an investigation of the intrusion of sea water into coastal aquifers. For this subject, this paper deals with proposing rational methods of getting diffusion coefficient and dispersion parameter for flow in porous media in a laboratory. These parameters of soil are indispensable in order to apply an analytical approach or a numerical approach to actual salt water intrusion problems. Experimental apparatuses were constructed and test procedures were also developed to measure concentration behaviors in a saturated porous media by using electro conductivity probe. As the results, the diffusion coefficients for the Toyoura standard sand and the Asahi river sand determined by two methods, that is, "Boltzman's transformation method" and "Instantaneous profile analysis method". The longitudinal coefficient of dispersion for one-dimensional flow was also determined by the least squares curve fitting method with a function of a certain range of seepage velocity.

* Department of Civil Engineering

1. Introduction

As increasing usage of fresh ground water supplies in coastal regions, the dynamic balance between the fresh ground water flow to the saline ocean water becomes instable. This imbalance has been observed in the pollution of fresh water by brackish water. This phenomenon has frequently happened due to the drawdown of ground water in order to excavate grounds near the ocean. The phenomenon of salt water wedge advancing inland is called "salt-water intrusion". The earliest studies of this subject were made in the northern coastal region of Europe. The well-known Ghyben-Herzberg (1889-1901) static equilibrium principle was the first formulation for the extent of saline intrusion. Since that time various studies have been made, both theoretical and experimental. The discussion of seawater intrusion models can be presented separately for fully mixed models and sharp interface models. The type of model concerns the way the transition zone between freshwater and seawater is treated. In reality, freshwater and seawater are two miscible fluids, with a transition zone between them. In this zone dispersive mixing occurs between the two fluids. Often this transition zone is very thin, compared with the aquifer thickness. When this occurs, an abrupt or immiscible interface between freshwater and seawater usually is assumed [1,2]. Different equation are solved for different "types of models". A fully mixed model requires the coupling of two equations: the flow equation and the mass transport equation. A sharp interface model requires the solution of two flow equations: one for freshwater, the other for seawater.

To evaluate which model is better, it is necessary to investigate a spread of a transition zone. With the advent of high speed digital computers numerical models have become an attractive solutions method for problems that are too complicated to solve analytically [3,4,5]. Many complicated seawater intrusion problems with full mixed model can be solved by applying finite element method. However, the reliability of the results obtained by this method depends largely on the accuracy of the numerical values of the hydraulic and dispersion characteristics of aquifers. It is obvious that the result of any seawater intrusion computation will be erroneous when

these values are insufficiently known. In order to investigate the validity and the accuracy of the numerical analysis solution, in general two methods are used, i.e., numerical results are compared with the analytical results of simple problems for which rigorous analytical solutions are available and numerical results are compared with the experimental results. As far as authors know, there are only few the experimental results on this subject, and there is no research on comparing numerical results with experimental results for seawater intrusion problems with the full mixed model.

The purposes of this paper are to propose rational methods of getting diffusion and dispersion parameter for flow in porous media in a laboratory test. These parameters of soil are indispensable to apply an analytical approach or a numerical approach to actual salt water intrusion problems.

2. Theory

2.1 Analysis of Determining Diffusion coefficient

(1) Boltzman's transformation method

In one-dimension, the equation describing the movement of solution in a saturated homogeneous soil is

$$\frac{\partial c}{\partial t} = \frac{\partial}{\partial z} (D(c) \frac{\partial c}{\partial z}) \quad (1)$$

where c is concentration of diffusion mass, z is the distance, and $D(c)$ is the diffusion coefficient. If we assume uniform initial concentration and a constant concentration at the boundary of a semi-infinite slab, the initial and boundary conditions are

$$\left. \begin{array}{l} c=0, \quad x>0, \quad t=0 \\ c=c_0, \quad x=0, \quad t>0 \end{array} \right\} \quad (2)$$

The Boltzmann transformation, $\lambda = z/\sqrt{t}$ when substituted into equation (1) reduces it to an ordinary differential equation [6]

$$-\frac{1}{2} \lambda \frac{dc}{d\lambda} = \frac{d}{d\lambda} \{ D(c) \frac{dc}{d\lambda} \} \quad (3)$$

with the boundary conditions

$$\left. \begin{array}{l} c=0, \quad \lambda \rightarrow \infty \\ c=c_0, \quad \lambda=0 \end{array} \right\} \quad (4)$$

It is convenient to consider the integral of (3) namely,

$$-\frac{1}{2} \int_0^c \lambda dc = D(c) \frac{dc}{d\lambda} \quad (5)$$

From above equation, the diffusion coefficient is given by

$$D(c) = \frac{-\int_0^c \lambda dc}{2 \left(\frac{dc}{d\lambda} \right)} \quad (6)$$

The numerator in equation (6) can be obtained by integrating graphically with respect to $c-\lambda$ profile curve, as shown in Fig.1. This curve may be differentiated graphically to give the concentration gradient ($\partial c / \partial \lambda$) .

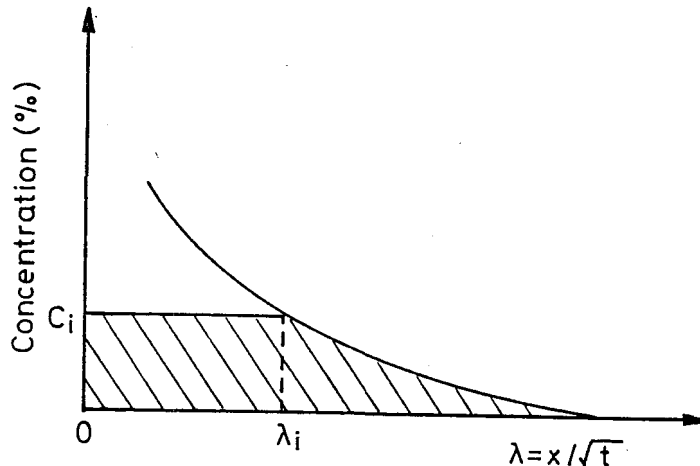


Fig.1 Functional relationship between concentration and $\lambda (=x/\sqrt{t})$

(2) Instantaneous Profile Analysis method [7]

The method of instantaneous profiles consists of determining the profiles of the macroscopic concentration flow velocity, the concentration gradient at any instant of time after the commencement of diffusion test.

Integration of Eq.(1) with respect to z yields:

$$\int \frac{\partial c}{\partial t} dz = D(c) \frac{\partial c}{\partial z} + C_1(t) \quad (7)$$

It should be noted the velocity is zero at the column upper boundary as sketched in Fig.2, then Eq.(7) becomes

$$\int_{z_0}^z \frac{\partial z}{\partial t} dz = D(c) \frac{\partial c}{\partial z} \quad (8)$$

From Eq.(8), it is a relatively simple matter to determine the instantaneous hydraulic conductivity for any elevation and time

$$D(c) = \frac{\int_{z_0}^z \frac{\partial c}{\partial t} dz}{\left(\frac{\partial c}{\partial z} \right)_{z,t}} \quad (9)$$

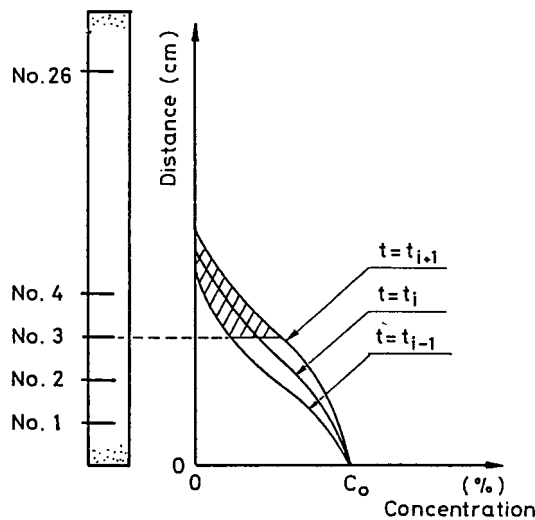


Fig.2 Relationships between concentration and distance

2.2 Analysis of Determining Dispersion

A one-dimensional dispersion model for a homogeneous porous medium can be obtained by a mass balance:

$$\frac{\partial c}{\partial t} = D' \frac{\partial^2 c}{\partial z^2} - v \frac{\partial c}{\partial z} \quad (10)$$

where D' is the longitudinal dispersion coefficient, v is seepage velocity, and z is distance in a Cartesian coordinate system. The solution of Eq.(10) for a step input has been reported for several sets of boundary conditions. The semi-infinite boundary conditions and initial condition are

$$\left. \begin{array}{ll} c(0,t) = c_0 & t \geq 0 \\ c(\infty,t) = 0 & t \geq 0 \\ c(z,0) = 0 & z \geq 0 \end{array} \right\} \quad (11)$$

where c_0 is inlet concentration. The solution to this equation with the indicated boundary and initial conditions has been given as [8]

$$\frac{c}{c_0} = \frac{1}{2} \operatorname{erfc}\left(\frac{z-vt}{2\sqrt{Dt}}\right) + \frac{1}{2} \exp\left(\frac{Vz}{D'}\right) \operatorname{erfc}\left(\frac{z+vt}{2\sqrt{Dt}}\right) \quad (12)$$

where $\operatorname{erfc}(x)$ is the complementary error function, i.e.,

$$\operatorname{erfc}(x) = 1 - \operatorname{erf}(x) \quad (13)$$

It can be shown that the second term of Eq.(12) can be neglected when (D'/Vz) is less than one. With the second term neglected, Eq.(12) can be written in dimensionless form as

$$\frac{c}{c_0} = \frac{1}{2} \operatorname{erfc}(\xi) \quad (14)$$

where

$$\xi = \frac{(z-vt)}{\sqrt{4Dt}} \quad (15)$$

The numerical result of Eq.(14) is shown in Fig.3. For the solution given in Eq.(14), the quantity ($2c/c_0$) can be computed from experimental measurements for each value of time, t_i and each value of elevation, z_i . Thus ξ can be determined from tables of the complementary error function or graphical representation of this function. Eq.(15) can be rewritten as

$$D'_i = \frac{1}{4} \frac{(z - Vt)^2}{\xi^2 t_i} \quad (16)$$

The longitudinal dispersion coefficient, D'_i , can be calculated from Eq.(16) for each values of t and z . By using method of least squares, the mean longitudinal dispersion coefficient, D' , can be obtained as the function of V from next equation,

$$D' = \frac{1}{4} \left(\frac{\sum \xi_i (z_i - Vt_i) \sqrt{t_i}}{\sum \xi_i^2 t_i} \right)^2 \quad (17)$$

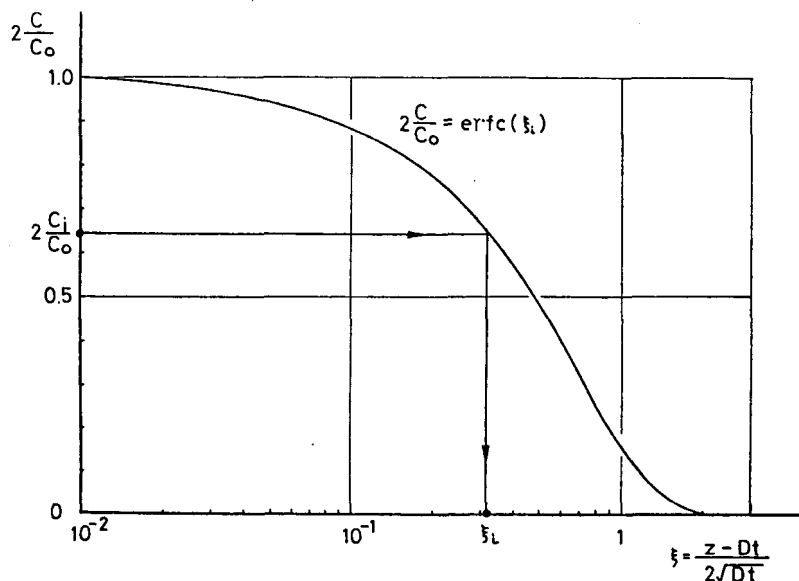


Fig.3 Numerical solution of $\text{erfc}(\xi)$

3. Experimental Equipment and Procedure

3.1 Diffusion

(1) Column

The longitudinal diffusion tests were performed in an acrylic cylinder with an inside diameter of 5.4cm (see Fig.4). A thin stainless steel mesh filter and a porous plate at the top and bottom respectively were used to contain the porous medium in the column. The length of the test section is the column was 70.0cm. Provisions for conductivity probes were located every 2.5cm. All water to be used in the column tests was first deaerated by circulating through a vacuum tank. During the course of experiments, air was never detected in the column. In order to avoid entrapment of air in the sand while filling the column, the desicator was first filled with water and dry sand was then poured at a slow rate into the desicator so that each grain fell separately and air could easily escape. After this process, to ensure further removal of entrapped air in the sand the vacuum pump was connected with the desicator.

(2) Materials

The soil samples used in this experiment were Toyoura standard sand and the Asahi river sand. Each grain size accumulation curves for these sand are shown in Fig.5. The materials were carefully packed into the acrylic cylinder column from the desicator. The porosity of the standard sand was 0.390, and that of the river sand was 0.397.

(3) Tracer substance

A solution of 3 per cent by weight NaCl was used as the tracer solution. At this concentration, the conductance of the electrolytic solution varies linearly with concentration, thus simplifying the calibration of the conductivity probes.

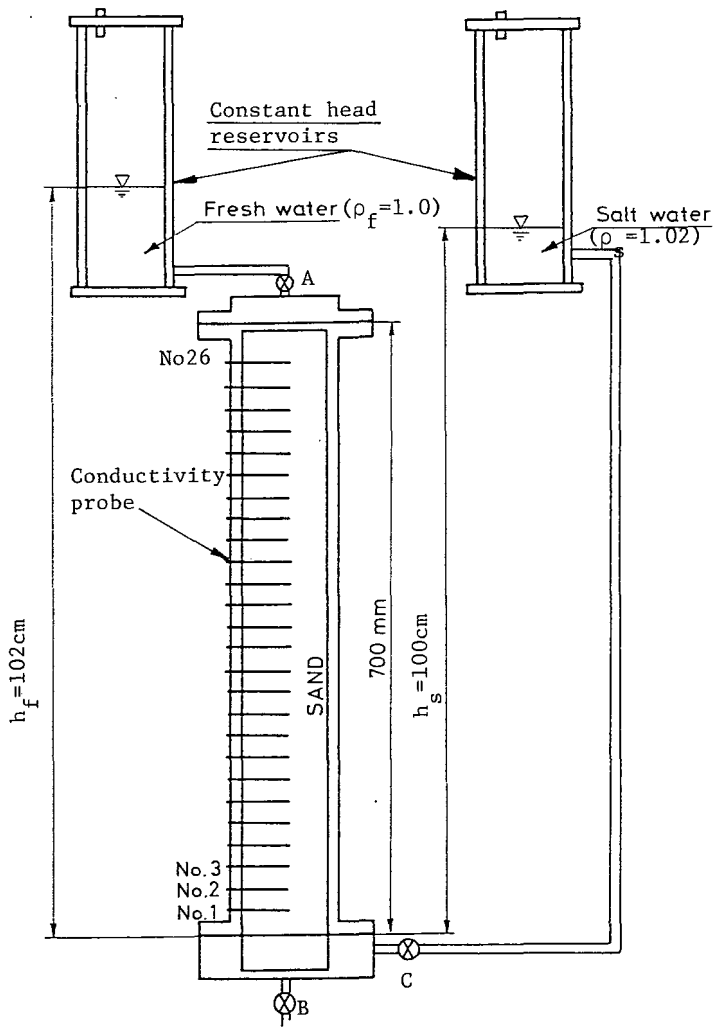


Fig.4 Schematic diagram of the diffusion apparatus

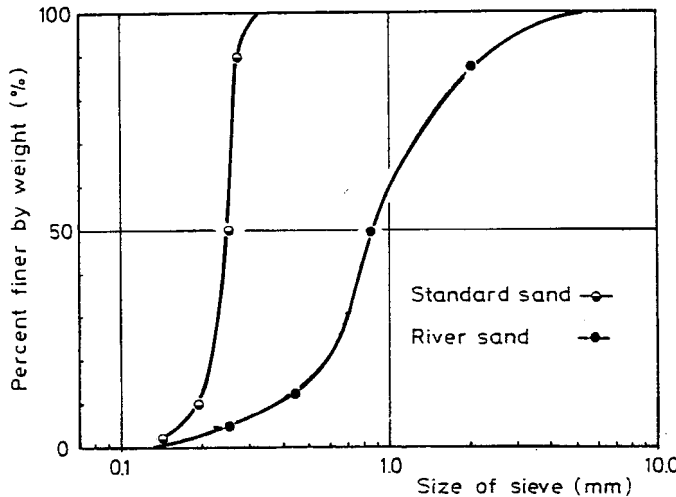


Fig.5 Grain size accumulation curves for standard sand and river sand

(4) Conductivity probe

Conductivity probe method of measuring electrical conductivity of the soil eliminates time lag but introduces the problem of correcting the changes in conductivity with varying concentration of the soil water. This method has been used on much larger scale by geophysicists to measure the resistivity of earth and rocks tested this method as possible procedure to measure soil water content. A highly significant linear relationship was found between specific electrical conductivity and concentration of solution in soil water. In this experiment, the conductivity probe consisted of insulated copper wire which were let to copper electrodes as sketched in Fig.6. The position of the probe in the column can be see in Fig.4.

By filling the column with various concentrations of salt solutions and independently recording the conductance, a calibration curve was determined for the probe. The variable of the dependence of solution conductance on temperature was also revised in the various temperature tests. Fig.7 shows the relations between conductance and temperature for parameter of concentration. Fig.8 also shows the relations between alternating current (AC) and concentration (c) for electrode point 1.

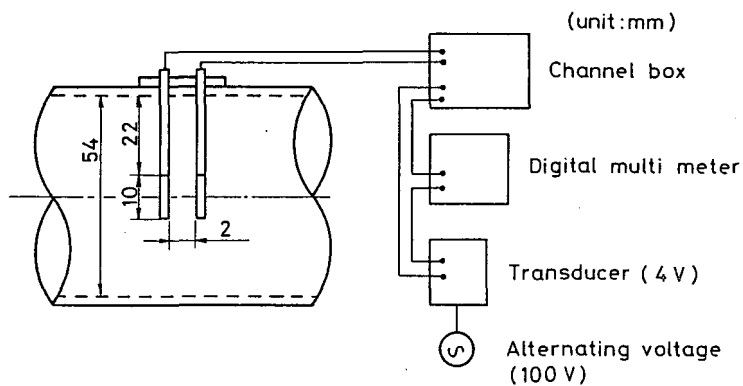
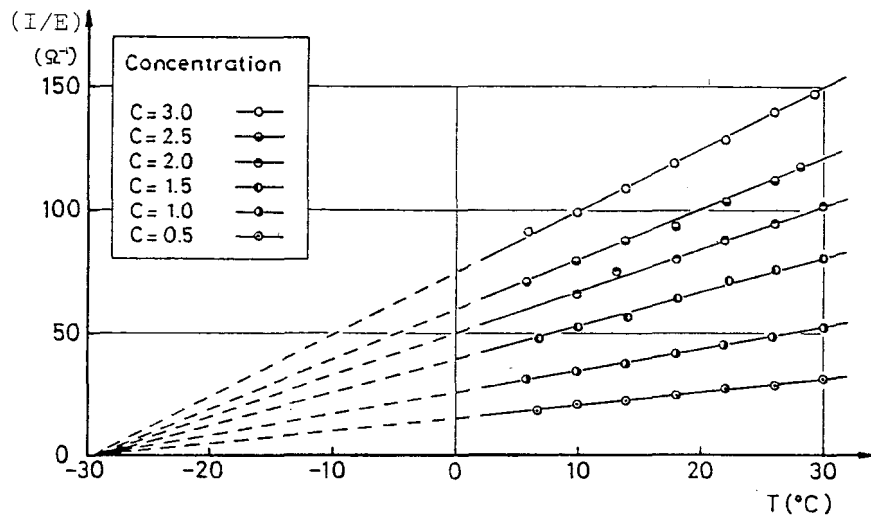


Fig.6 Schematic diagram of the electrode arrangement

Fig.7 Relation between conductance (I/E) and temperayure (T) for parameter of concentration

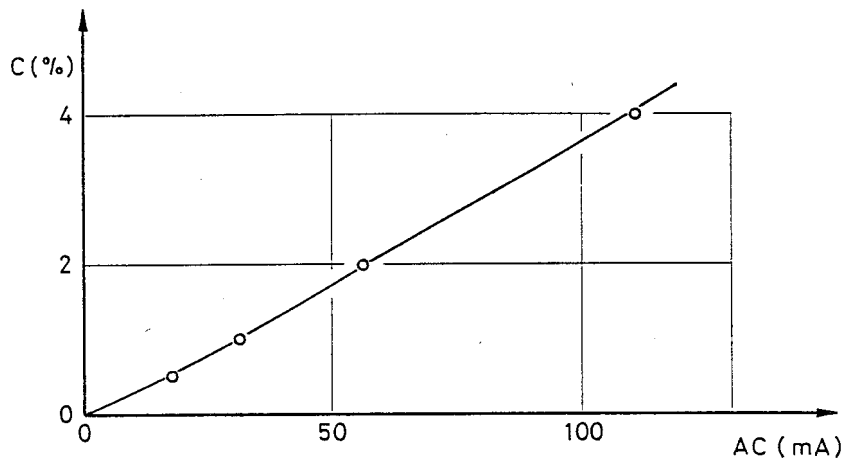


Fig.8 Relation between alternating current(AC) and concentration (c) for electrode point 1

(5) Procedure

The packed column was saturated with fresh water ($t < 0$). The constant head reservoir of fresh water was connected to the column. In this condition the reservoir at the bottom of the column was also filled with fresh water. At time, $t=0$, the predetermined valves, B and C (see Fig.4) were opened, and the reservoir at the bottom of the column was filled with salt water. After this process, immediately the valve B was closed. The head level of fresh water and that of salt water were kept at 102cm and at 100cm respectively. These head levels were determined from the reason that the specific gravity of fresh water is $\rho_f = 1.0$ and that of salt water of 3 per cent concentration is $\rho_s = 1.02$. Then at the bottom of sand column, the pressure of fresh water was in equipose with that of salt water. Periodic measurements of alternating current were recorded.

3.2 Dispersion

(1) Apparatus

The same procedure as outlined for the diffusion was repeated in this dispersion experiment. The schematic diagram

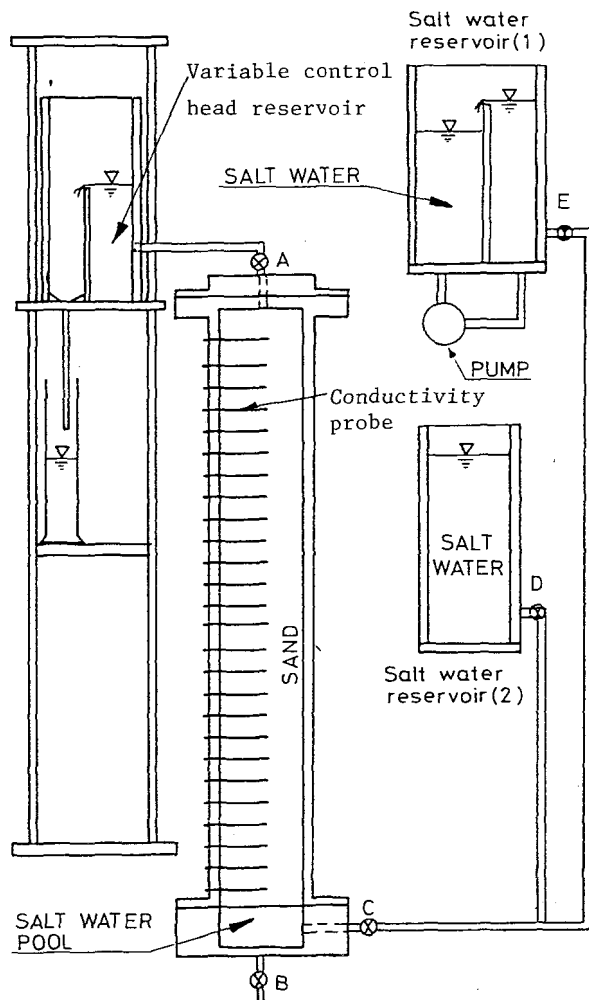


Fig.9 Schematic diagram of the dispersion experimental equipment

of the dispersion experimental equipment is shown in Fig.9. This apparatus was used throughout this study.

(2) Procedure

The sand column was first saturated with the fresh water and then valves C, B (see Fig.9) were opened. After salt water filling the reservoir at the bottom of the column, the valve B was closed. A front of salt water was translated through the model causing a transition zone to develop. To investigate an effect of seepage velocity on the dispersion, this experiments were performed in the condition of various seepage velocity as described in Table 1. The flow rate could be adjusted by changing the reservoir box height at the outlet. The flow was measured by means of a volumetric tank. The vertical profiles of tracer concentration were measured at the twenty-six stations.

Table 1 Average pore velocity

V (cm /sec)
1.43×10^{-3}
4.30×10^{-3}
1.02×10^{-2}
1.62×10^{-2}
2.54×10^{-2}
3.92×10^{-2}
4.02×10^{-2}

4. Experimental Results and Discussion

4.1 Diffusion

The results relative to the diffusion test are reported in Fig.10 and Fig.11. Fig.10 and 11 indicate the vertical profiles of the tracer concentration at different time for the standard sand and the Asahi river sand respectively. From these results the relations between concentration (c) and Boltzman's transformation parameter (λ) are easily obtained by the method of previous section 2.1, as shown in Fig.12, 13. As the results, the diffusion coefficients for the standard sand and the Asahi river sand are plotted in Fig.14 and Fig.15 with respect to concentration. As it is clear from Fig.14 and Fig.15 that the diffusion coefficient is not dependent on the concentration. For reference the diffusion coefficient of solution without porous media are shown in Fig.14, 15. These coefficient are

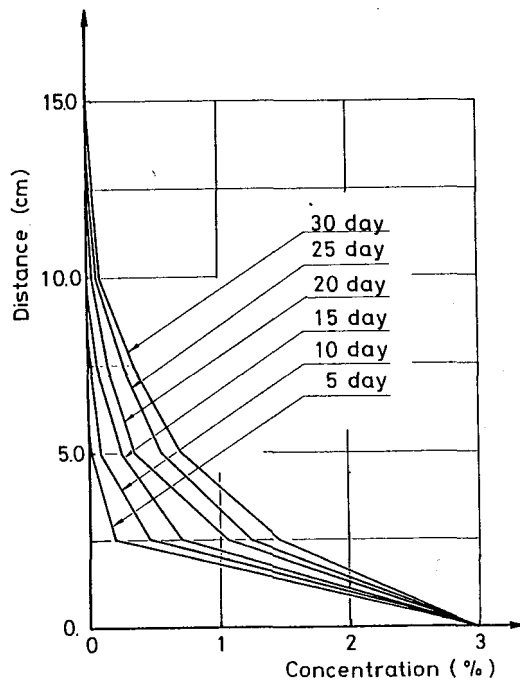


Fig.10 Observed NaCl profiles for standard sand

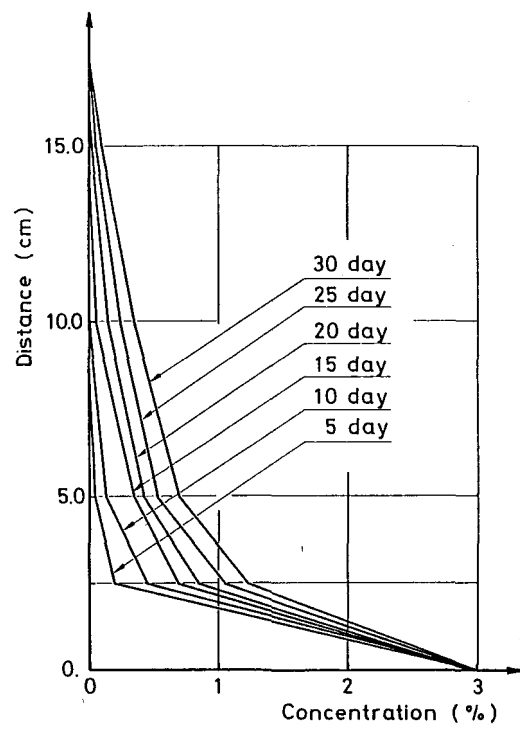


Fig.11 Observed NaCl profiles for river sand

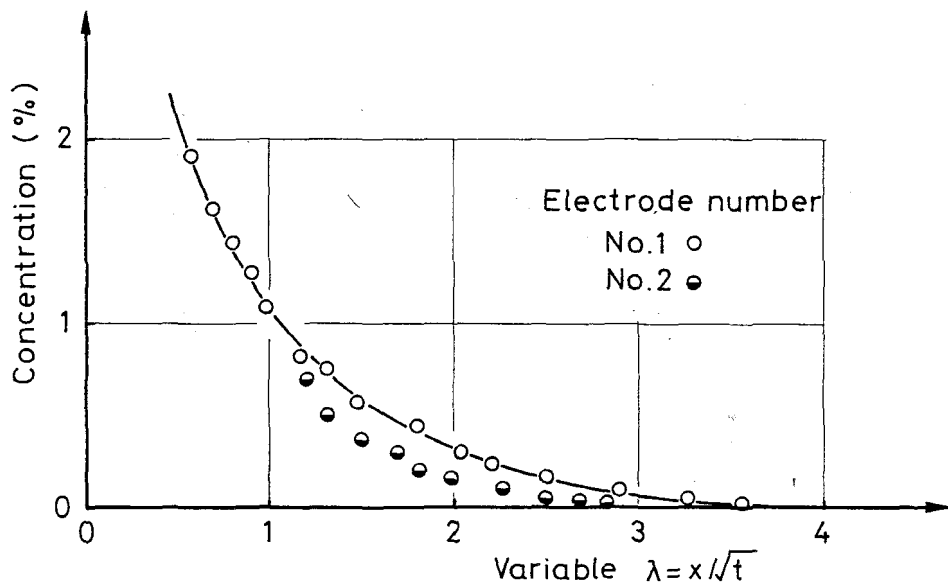


Fig.12 Experimental results of concentration and $\lambda (=x/\sqrt{t})$ for standard sand

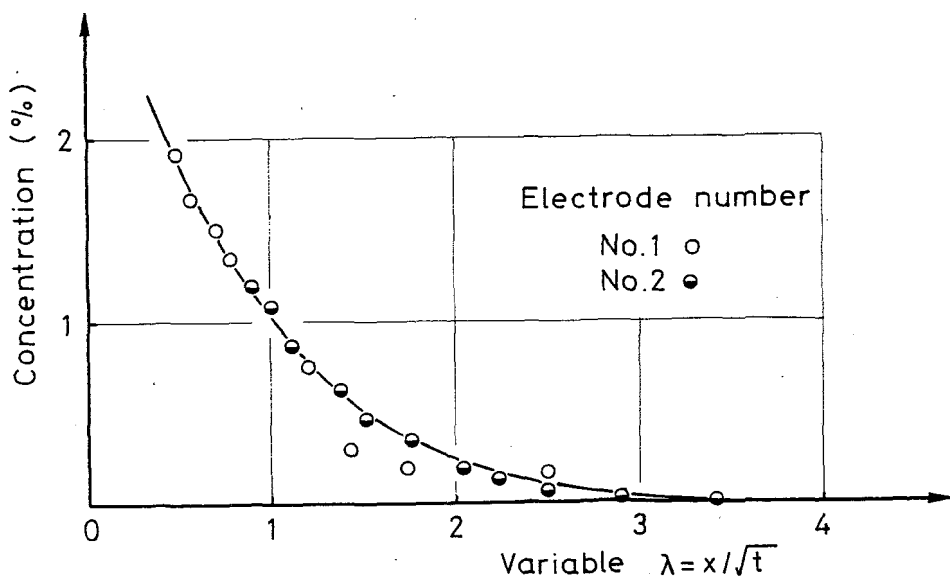


Fig.13 Experimental results of concentration and $\lambda (=x/\sqrt{t})$ for river sand

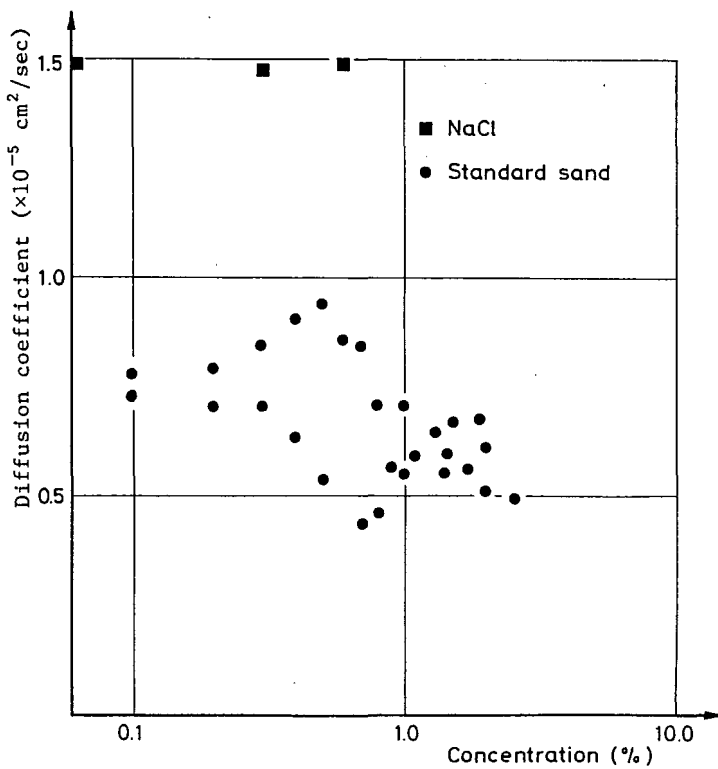


Fig.14 Relationship between diffusion coefficient and concentration for standard sand by Boltzmann Method

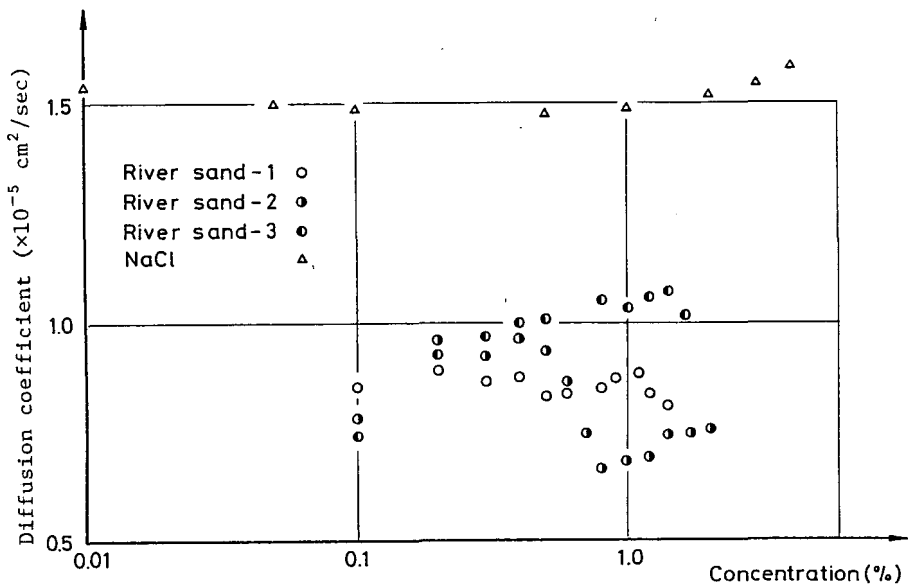


Fig.15 Relationship between diffusion coefficient and concentration for river sand by Boltzmann Method

also independent of the solution concentration. Fig.14 clearly shows that the diffusion coefficient without porous medias are larger than the ones obtained with porous medias. The reason of this difference may be explained as follows. Diffusion coefficients are generally defined in terms of mass flux across a unit area. In a porous medium the area across which molecular diffusion takes place varies for the larger irregular pore openings to the smaller connecting channels. Also the direction of the mass flux is continually changing, since this would be governed by the local concentration gradients across the individual pores and channels. Thus a diffusion coefficient is defined for a porous medium. This coefficient is a function of the fluid, the temperature, the concentration of the tracer substance in the liquid, and the pore system geometry of the media. And also this coefficient must be determined experimentally. The mean values of the diffusion coefficient obtained in these experiments are given in Table 2 with the values obtained by the end cap break-through curves method for various size of glass beads [9]. It is obvious in Table 2 that the diffusion coefficient increased with the grain size. Fig.16, 17 show the diffusion coefficients for the standard sand and the Asahi river sand obtained by the instantaneous profile Analysis method.

Table 2 Diffusion coefficient for various porous media

Media	Diffusion coefficient (10^{-6} cm/sec)
solution	15.0
the standard sand mean size(d_{50}) 0.25mm	6.3
the Asahi river sand mean size(d_{50}) 0.88mm	8.8
glass beads effective size 0.10mm	5.7
glass beads effective size 0.30mm	7.8
glass beads effective size 1.00mm	9.5

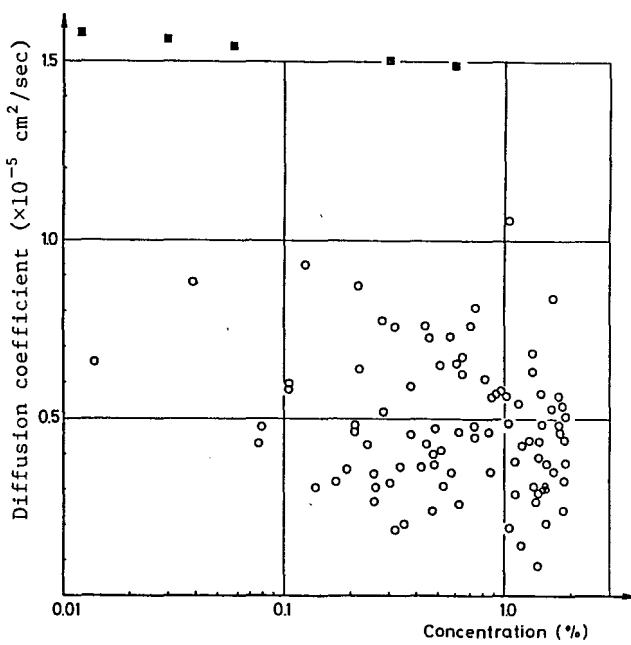


Fig.17 Relationship between diffusion coefficient and concentration for river sand by Profil Method

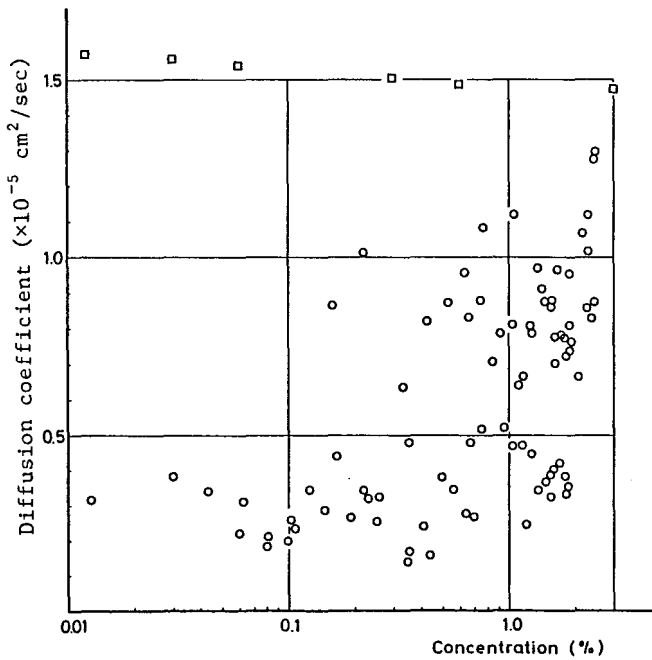


Fig.16 Relationship between diffusion coefficient and concentration for standard sand by Profil Method

4.2 Dispersion

One dimensional concentration, C, was recorded as a function of time at the twenty-six conductivity probes, for specified values of the seepage velocity. Typical results for this test can be seen in Fig.18. From these concentration profiles, experimental curves of c/c_0 versus ($z-Vt$) is shown in Fig.19. One can easily understand the transition zone spreading with time. By the method of previous section 2.2, for each seepage velocity studied, the dispersion coefficient for the standard sand were obtained as listed in Table 3.

The dispersion coefficients and velocity are generally correlated by the dispersivity model

$$D = aV^b \quad (18)$$

where a and b are constants determined experimentally. By using method of least squares, a and b were determined to be 0.398 and 1.471 respectively, thus Eq.(18) can be written for the standard sand as

$$D = 0.398V^{1.471} \quad (19)$$

For the Asahi river sand, the constants in Eq.(18) were also determined and Eq.(18) can be also written as

$$D = 1.144V^{1.408} \quad (20)$$

Comparisons of the experimental results and regression equations are shown in Fig.20.

Another model used for correlating the dispersion coefficients and Reynolds numbers (Reynolds number are defined using the seepage velocity, the 50 per cent grain size (d_{50}), and the Kinematic viscosity (ν) of fresh water) is

$$\frac{D}{\nu} = \alpha Re^\beta \quad (21)$$

Table 4 shows the result of this experiment and previous works. As Table 4 indicates, the value of α varies from 0.2 to 4.0, but the range of parameter β is 0.98~1.47. It should be noted

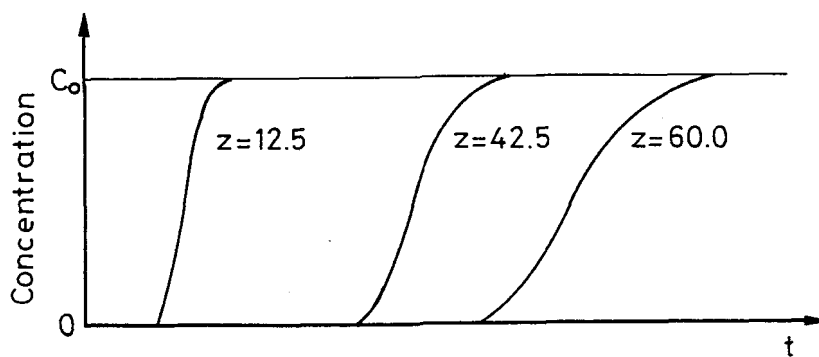


Fig.18 Experimental results of concentration versus time at various distances (z) ($V=3.98 \times 10^{-2}$ cm/sec)

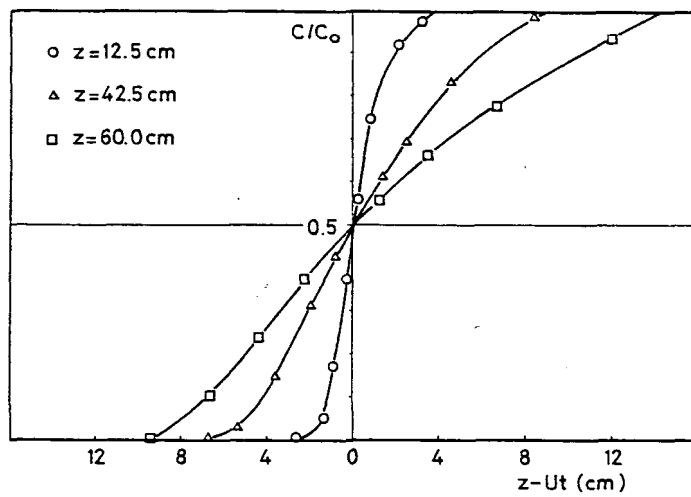


Fig.19 Concentration profiles for dispersion test in standard sand ($V=3.98 \times 10^{-2}$ cm/sec)

Table 3 Dispersion coefficient for various velocity

V (cm/sec)	D (cm ² /sec)	Re	L (cm)
1.43x10 ⁻³	3.27x10 ⁻⁵	4.29x10 ⁻³	12.5
"	3.95x10 ⁻⁵	4.29x10 ⁻³	42.5
"	3.59x10 ⁻⁵	4.29x10 ⁻³	60.0
4.30x10 ⁻³	6.41x10 ⁻⁵	1.29x10 ⁻²	12.5
"	9.23x10 ⁻⁵	1.29x10 ⁻²	42.5
"	8.09x10 ⁻⁵	1.29x10 ⁻²	60.0
1.02x10 ⁻²	4.41x10 ⁻⁴	3.06x10 ⁻²	12.5
"	3.45x10 ⁻⁴	3.06x10 ⁻²	42.5
"	5.01x10 ⁻⁴	3.06x10 ⁻²	60.0
1.62x10 ⁻²	5.67x10 ⁻⁴	4.86x10 ⁻²	12.5
"	1.38x10 ⁻³	4.86x10 ⁻²	42.6
"	1.95x10 ⁻³	4.86x10 ⁻²	60.0
2.54x10 ⁻²	9.31x10 ⁻⁴	7.62x10 ⁻²	12.5
"	1.67x10 ⁻³	7.67x10 ⁻²	42.5
"	3.73x10 ⁻³	7.67x10 ⁻²	60.0
3.92x10 ⁻²	2.30x10 ⁻³	1.19x10 ⁻¹	12.5
"	4.66x10 ⁻³	1.19x10 ⁻¹	42.5
"	7.92x10 ⁻³	1.19x10 ⁻¹	60.0
4.02x10 ⁻²	2.14x10 ⁻³	1.21x10 ⁻¹	12.5
"	6.13x10 ⁻³	1.21x10 ⁻¹	60.0

V:Velocity D:Dispersion coefficient Re:Reynolds
 number L:Distance to probe

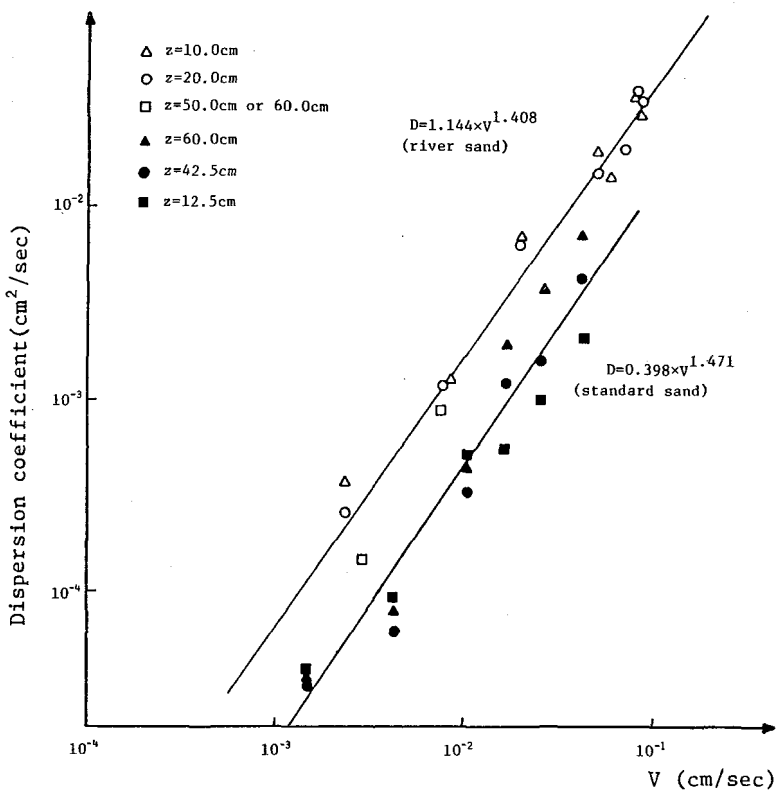


Fig. 20 Relation between dispersion coefficient and pore water velocity

Table 4 Disersion coefficient

Madia	$d_{50\text{mm}}$	D/V
the standard sand	0.32	$0.26Re^{1.47}$
the stansard sand [9]	0.32	$0.11Re^{0.989}$
sand [10]	2.2	$0.85Re^{1.40}$
sand [10]	0.56	$3.60Re^{1.40}$
quartz gravel [11]	1.65	$0.86Re^{1.14}$
glass beads [11]	0.39	$0.63Re^{1.14}$
plastic spheres [12]	0.96	$0.66Re^{1.20}$
glass beads [15]	1.00	$1.00Re^{1.21}$
glass beads [9]	1.00	$1.70Re^{0.989}$

that for Reynolds number less than 10^{-3} the seepage velocity becomes so small that the influence of diffusion becomes important. When the parameters α , β of Eq.(21) were compared for the standard sand in Table 4, there was difference in these values. The reason may be the difference in bulk densities. The porosity in this experiment was 0.397, and that in reference [9] was 0.415.

5. Conclusions

- (1) Two method were used for determining the diffusion coefficient as a function of concentration.
- (2) This method has the advantage of being an instantaneous reading which is adapted for quick measurements of dispersion of soils.
- (3) The experimentally determined dispersion coefficient were obtained from break through curves generated by upward miscible displacement in vertical columns of the standard sand and the Asahi river sand.
- (4) The values of the dispersion parameters were obtained by method of least squares for both sands.

Acknowledgement

The authors wishes to express their sincere thanks to Mr. M. Hirano of Aichi prefectural office for his assistance during various periods of the experimental study.

References

- [1] J. Bear : Dynamics of Fluids in Porous Media, Elsevire, (1972).
- [2] I. Kohno : Analysis of interface problem in groundwater flow by finite element method, Finite Element Methods in Engineering, the University of New South Wales, (1974), 815-825.
- [3] U. Shamir and G. Dagan : Motion of the seawater interface

- in coastal aquifers, a numerical solution, Water Res. Res., 7(3) (1971), 644-657.
- [4] G. F. Pinder and R. H. Page : Finite element simulation of salt water intrusion on the South Fork of Long Island, presented at the International Conference in Finite Elements in Water Resources, Princeton, (1976).
 - [5] G. F. Pinder and R. H. Gray : Finite Element Simulations in Surface and Subsurface Hydrology, Academic Press, New York, (1977).
 - [6] J. Crank : The mathematics of diffusion, Oxford at the Clarendon press, (1955), 148-149.
 - [7] I. Kohno and M. Nishigaki : Experimental study on determining unsaturated property of soil, Memoirs of the School of Engineering, Okayama University, 14(2) (1980), 73-110.
 - [8] Ogata, A., Dispersion in porous media, Ph. D. thesis, Northwestern University, Chicago, III., (1958).
 - [9] M. Fukui and K. Katsurayama : Study on the phenomena of molecular diffusion and dispersion in saturated prous media, Proc. JSCE, 246 (1976), 73-82 (in Japanese).
 - [10] Chikasui handbook, (1979), 105, (in Japanese).
 - 11) R. R. Rumer, Jr. : Longitudinal dispersion in steady and unsteady flow, ASCE, 88(HY4) (1962), 147-171.
 - 12) R. R. Rumer, Jr. and D. R. F. harleman : Intruded salt-water wedge in porous media, ASCE, 89(HY6) (1963), 193-220.
 - 13) T. Ohoro and K. Suzuki : Study on dispersion in porous media, Regional Anual meeting of JSCE, (1979), 134-135, (in Japanese).
 - 14) S. Kazita and K. Suzuki : Study on dispersion in porous media, Regional Anual meeting of JSCE, (1980), 55-56, (in Japanese).